Purdue University
Purdue e-Pubs

International Refrigeration and Air Conditioning Conference

School of Mechanical Engineering

2018

Model-Based Performance Comparison of Ammonia Chemisorption Heat Pumps for Cold Climate with Different Working Pairs and Cycle Configurations

Zhiyao Yang
"Purdue University, United States of America; Oak Ridge National Laboratory, United States of America",
yang573@purdue.edu

Ming Qu
Purdue University, mqu@purdue.edu

Kyle Gluesenkamp
Oak Ridge National Laboratories, United States of America, gluesenkampk@ornl.gov

Follow this and additional works at: https://docs.lib.purdue.edu/iracc

Model-Based Performance Comparison of Ammonia Chemisorption Heat Pumps for Cold Climate with Different Working Pairs and Cycle Configurations

Zhiyao YANG[1,2], Ming QU[1]*, Kyle GLUESENKAMP[2]

[1]Purdue University, Lyle School of Civil Engineering, West Lafayette, Indiana, USA

[2]Oak Ridge National Laboratory, Oak Ridge, Tennessee, USA

* Corresponding Author: mqu@purdue.edu

ABSTRACT

Space heating is a major contributor to building energy consumption especially in cold climates. Conventional gas-fired furnaces are approaching thermodynamic efficiency limits, while electric heat pumps performance declines drastically at low ambient temperature. Chemisorption heat pump (CSHP) systems could be a better solution to space heating for cold climate due to their sustained capacity and efficiency at large temperature lifts. The performance of CSHP primarily depends on the working pair and cycle configuration. Most existing comparative studies of chemisorption systems in the published literature focus on refrigeration, but not many in heating applications. The few existing studies of chemisorption heat pump for heating involved too limited cycles and working pairs to represent the most promising performance of the CSHP. The goal of this study is to fill the gap through extensive performance comparison of CSHP using various salts and cycle configurations to discover the potential in space heating of the CSHP technology. Thermodynamic models of six cycle-configurations were first developed and applied to evaluate system performances across the 65 working pairs operated at cold climate heat pumping conditions. The system performances were predicted and compared under different ambient temperatures and assumed system design parameters such as thermal masses. The comparison shows that the double-effect CSHP has the highest efficiency at ambient temperature below -20°C with cycle thermal Coefficient of Performance (COP) above 1.5 and system primary energy COP above 1.2.

1. INTRODUCTION

Space heating contributed to more than 45% of energy consumption in residential buildings in U.S. (DOE 2012), while the heating energy consumption is even higher in cold climates. Therefore, improving the energy efficiency of space heating equipment has significant energy saving potential. Conventional gas-fired furnaces produce heat at constant efficiency regardless of the ambient temperature. However, these gas-fired systems have already approached their ideal thermodynamic efficiency of 1 with very limited potential for improvement. Electric heat pumps can operate with high performance in mild climates, but their primary energy efficiencies decline drastically at low ambient temperature.

Thermally-driven ammonia-based chemisorption heat pumps (CSHP) have the potential to provide space heating with high energy efficiency in cold climates. In a CSHP, ammonia vapor is adsorbed or desorbed on the solid sorbent surface through reversible chemical reactions, and the associated reaction heat is used for heat extraction from the ambient or heat supply to the buildings. The thermal efficiency of CSHP exceeds the theoretical limit of gas-fired furnaces; meanwhile, this efficiency is sustained at low ambient temperature due to the mono-variant vapor

equilibrium of chemisorption reactions. The design of a CSHP involves selecting from the numerous available sorbent salts and cycle configurations, and such selections largely determine the coefficient of performance (COP) of the CSHP. Therefore, comparison of different salt and cycle options is necessary for proper design of CSHPs.

Several existing studies found in literature compared the COP for chemisorption systems using different sorbent salts and cycle configurations. Goetz et al. (1993) compared the performance of single-effect chemisorption systems for refrigeration and thermo-transformation using 26 ammoniate salt and single-stage adsorption configuration and resorption configurations. Wang et al. (2009) compared the performance of these two single-stage configurations in deep freezing applications using three different salts. Neveu and Castaing (1993) investigated the performance of a double-stage chemisorption refrigeration cycle. A domain of application was generated from the model results of 16 ammoniate salt, where the estimated COP and required heat source temperature were correlated with the evaporation temperature. Li et al. (2009) compared the performance of chemisorption refrigeration systems using single-effect, double-effect, and triple-effect cycle configurations. Two different salts and salt combinations were used for single and double stage cycle, and one salt combination was used for triple stage. In a study by Pons et al. (1999), five ammonia-based chemisorption systems using four salts and four cycle-configurations were included in the thermodynamic performance comparisons of 22 thermally-driven sorption systems for air conditioning, refrigeration, and heat pumping applications. The COP, heat source temperature, specific heating/cooling power, and second law efficiency were evaluated for 22 systems and compared under different operating conditions.

Despite existing comparative studies, the heat pumping application of chemisorption systems as cold climate heat pumps has not been sufficiently explored: In studies focusing on refrigeration application, the heat rejection temperature is significantly lower than that in heat pump systems; in the few studies focusing on heat pumping application, the salts and cycle configurations considered were very limited compared to the available pool of candidates. Therefore, there is a gap in performance comparison of ammonia chemisorption systems for cold climate heat pumping. The goal of this study is to fill the gap and facilitate proper system design with the comparison results. In the following sections, the basic principles and cycle configurations of CSHPs are introduced; then a thermodynamic model for system performance evaluation is developed; finally, the COP of systems using six cycle configurations and 65 ammoniate salts under cold climate heat pumping conditions are compared and discussed.

2. BASIC PRINCIPLES OF CHEMISORPTION SYSTEMS

Chemisorption systems are based on the thermal effect of one or more reversible physicochemical reactions between a sorbent and a refrigerant gas: adsorption / synthesis / production and desorption / decomposition / regeneration. The thermal effect of ammonia chemisorption systems is generated through the reversible chemical reactions between ammonia vapor and the sorbent salt, which can be expressed in reaction formula (1). The pressure-temperature equilibrium of such a reaction is described by the van't Hoff relationship in equation (2) and illustrated on Clapeyron Chart as in Figure 1.

In the van't Hoff relationship, ΔH_r and ΔS_r are the enthalpy and entropy change associated to the reaction, R is the ideal gas constant, T is the temperature of sorbent in Kelvin, and P_{eq} is the corresponding equilibrium vapor pressure of ammonia in Pascal. Such equilibrium of a salt-ammonia reaction can be represented by a straight line in the Clapeyron chart. Figure 1 shows some commonly used reactions. The operating ranges of sorbent salts are determined by the temperature-pressure equilibrium, and therefore the Clapeyron chart can be used to select proper sorbents for CSHP design. For instance, when coupled with ammonia evaporator to produce heat at 50°C under ambient of -10°C, the salt should be able adsorb ammonia at temperature above 50°C while under the saturation pressure of ammonia at -10°C, as illustrated by the shaded area in Figure 1. In real systems, the sorbent salt is usually impregnated in porous matrix materials such as graphite and activated carbon to enhance the heat and mass transfer performance. This study includes 65 ammoniate reactions including metal chloride, bromide, and iodide, and their reaction enthalpy and entropy are listed in Neveu and Castaing (1993) and Li et al. (2014).
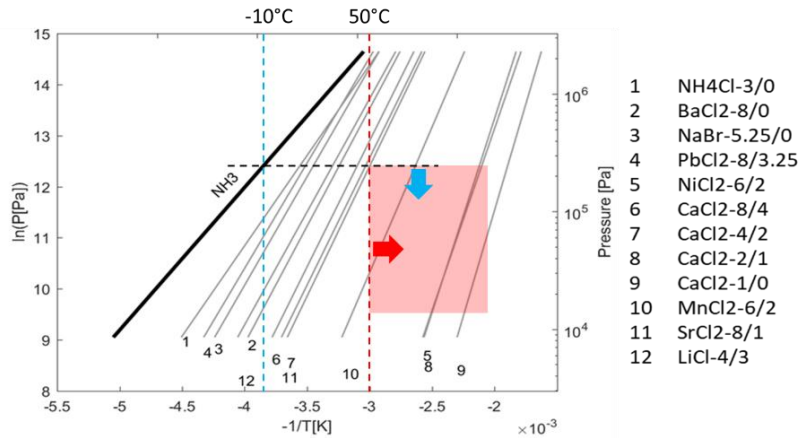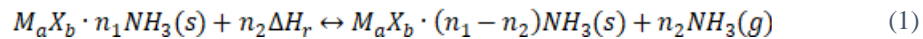
Figure 1: salt selection using reaction equilibrium lines on Clapeyron chart

$$M_aX_b \cdot n_1 NH_3(s) + n_2\Delta H_r \leftrightarrow M_aX_b \cdot (n_1 - n_2)NH_3(s) + n_2 NH_3(g) \tag{1}$$

$$\log P_{eq} = -\frac{\Delta H_r}{RT} + \frac{\Delta S_r}{R} \tag{2}$$

A wide variety of cycle configurations of chemisorption heat pump can be found in literature. In this study, the number of exchanger vessels including salt reactors and condensers/evaporators is limited to 4, leading to the available cycle configurations summarized in Table 1. Goetz et al. (1993) described the two most basic configurations: single-effect with NH_3 evaporator (SENE) cycle and single-effect resorption (SRES) cycle. SENE has one salt-containing reactor connected to a condenser and an evaporator, and it operates in two alternating half-cycles. SRES consists of two reactors containing two types of salts with different operating temperature ranges, and also operates in two alternating half-cycles. A variety of configurations based on these two basic cycles can be found in literature to improve the system performance. Heat-recovery (HR) mechanism was introduced to SENE by Wang et al (1998), and to double-effect resorption (DRES) by Oliveira et al. (2008). A double-effect cycle with NH_3 evaporator (DENE) was studied by Neveu (1993), and DRES cycles were investigated by Oliveira (2008).

For each configuration, the Clapeyron chart can be used to illustrate cycle operation with the equilibrium lines materials in the system as in Figure 2.
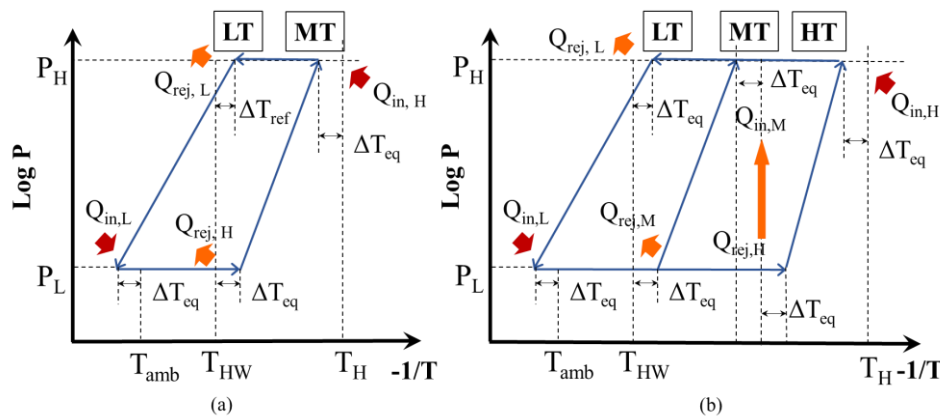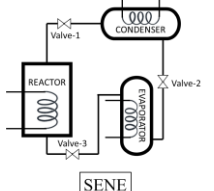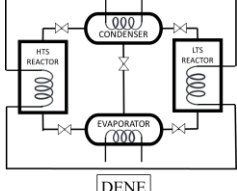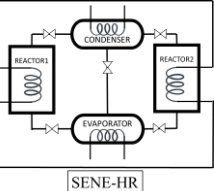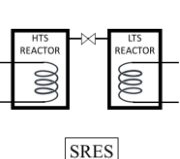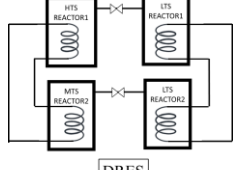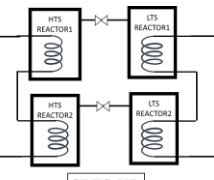

Figure 2: Chemisorption processes on Clapeyron chart a) Cycles of two: SENE, SENE-HR, SRES and SRES-HR and (b) Cycles of three: DENE and DRES

Figure 2 (a) shows the operation of SENE and SENE-HR with ammonia as the low temperature (LT) material and salt as the medium temperature (MT) material. Similarly, for SRES and SRES-HR Figure 2 (a) can be applied with LT as the LTS and MT as the HTS. The DENE and DRES cycles involve three different reactive materials, thus their operations can be described by Figure 2 (b), with LT representing the ammonia in DENE and the LTS in DRES, while the other two equilibrium lines represent two different salts. Besides the temperature and pressure levels of operation and the heat flow in each exchanger, Figure 2 also illustrates the equilibrium temperature drop necessary to drive chemical reaction. With given cycle configurations and physio-chemical properties of the working pairs, the performances of CSHP can be evaluated and compared using theoretical models.

Table 1: Summary of cycle configurations included in this study

Configuration	Heat recovery	Single-effect	Double-effect
NH₃ Evaporator	Non-HR	SENE	DENE
	HR	SENE-HR	N/A
Resorption	Non-HR	SRES	DRES
	HR	SRES-HR	N/A

3. THERMODYNAMIC MODEL

Chemisorption system operation is inherently transient, with varying heat flow and temperatures between the two half-cycles as well as within the same half-cycle as the chemical reaction progresses. However, chemisorption systems can still be analyzed using static models based on the overall thermodynamic performance over an entire cycle under simplifying assumptions (Goetz et al. 1993, Neveu and Castaing 1993, Wang et al. 2009). Such a thermodynamic model is agnostic to the working pair and is generic for each cycle configuration, and therefore suitable for comparing different system designs. In this study, static models have been developed to calculate and compare the heating COP of CSHP using six cycle configurations and various working pairs.

The heating COP is defined as the ratio of heat production over heat input. For CSHP cycles shown in Figure 2(a), the useful heat production ($Q_{out,THW}$) at supply temperature (T_{HW}) in an entire cycle includes adsorption heat ($Q_{rej,H}$) from reactors and condensation heat ($Q_{rej,L}$) from the condenser. The driving heat ($Q_{in,H}$) is the heat input at high temperature (T_H) into the salt reactor. With energy balance, the heating COP of CSHP can be expressed in equation (3) as one plus the ratio of heat extraction ($Q_{in,L}$) at low temperature (T_{amb}) over the driving heat, that is, one plus the cooling COP had it been used as a chiller.

$$COP_{ht} = \frac{Q_{out,T_{HW}}}{Q_{in,T_H}} = 1 + \frac{Q_{in,L}}{Q_{in,H}} = 1 + COP_{cl} \qquad (3)$$

Assuming for each salt there is only one stage of reaction, the ideal heat input and rejection in reactors and condenser/evaporator can be directly calculated using the ratio of salt reaction enthalpy ($\Delta H_{r,salt}$) and/or ammonia evaporation enthalpy (ΔH_{evap}) as listed in Table 2. In real systems, however, extra heat input is needed in every desorption half-cycle to heat the sorbent salt and matrix, ammonia, and reactor metal from post-adsorption medium temperature to high desorption temperature. Meanwhile, the pre-cooling of LTS and liquid ammonia from condensing/adsorption temperature to below ambient reduces the low-temperature heat extraction capacity.

There are inevitable and considerable energy losses due to the switches between the two half-cycles. Dead thermal mass (DTM), therefore, was introduced by Gluesenkamp (2012) introduced to reflect the losses. As shown in equation (4)-(6), the DTM, which is the product of the mass and specific heat, summed for all masses in the heat exchangers, for CSHP has two parts: *inherent DTM* (thermal mass of sorbent salt and retained ammonia), and *design DTM* (thermal mass of the sorbent matrix material and the reactor metal). The design DTM can be improved by optimizing the design of sorbent and exchangers, while the inherent DTM is intrinsic to the working pair.

$$DTM = DTM_{inherent} + DTM_{design} \qquad (4)$$

$$DTM_{inherent} = m_{salt} \cdot C_{p,salt} + m_{NH3} \cdot C_{p,NH3} \qquad (5)$$

$$DTM_{design} = m_{matrix} \cdot C_{p,matrix} + m_{metal} \cdot C_{p,metal} \qquad (6)$$

Introducing internal heat recovery mechanisms can reduce the effect of DTM by exchanging heat between corresponding reactors or evaporators between half-cycles. Table 2 also lists the COP expressions of six cycle configurations considering DTM. For heat recovery on the high-temperature and low-temperature side, heat recovery effectiveness ε_L and ε_H are defined respectively.

Table 2: Heating COP of investigated CSHP configurations

Cycle	Ideal Heating COP	Heating COP Considering Thermal Mass
SENE	$1 + \dfrac{\Delta H_{evap}}{\Delta H_{r,salt}}$	$1 + \dfrac{\Delta H_{NH3} - (T_{HW} - T_{amb}) \cdot DTM_{NH_3}}{\Delta H_{r,salt} + (T_H - T_{HW}) \cdot DTM_{reactor}}$
SENE-HR	$1 + \dfrac{\Delta H_{evap}}{\Delta H_{r,salt}}$	$1 + \dfrac{\Delta H_{NH3} - (T_{HW} - T_{amb}) \cdot DTM_{NH_3}}{\Delta H_{r,salt} + (1 - 0.5 \cdot \varepsilon_H) \cdot (T_H - T_{HW}) \cdot DTM_{reactor}}$
SRES	$1 + \dfrac{\Delta H_{r,LTS}}{\Delta H_{r,HTS}}$	$1 + \dfrac{\Delta H_{r,LTS} - (T_{HW} - T_{amb}) \cdot DTM_{LTS\ reactor}}{\Delta H_{r,HTS} + (T_H - T_{HW}) \cdot DTM_{HTS\ reactor}}$
SRES-HR	$1 + \dfrac{\Delta H_{r,LTS}}{\Delta H_{r,HTS}}$	$1 + \dfrac{\Delta H_{r,LTS} - (1 - 0.5 \cdot \varepsilon_L) \cdot (T_{HW} - T_{amb}) \cdot DTM_{LTS\ reactor}}{\Delta H_{r,HTS} + (1 - 0.5 \cdot \varepsilon_H) \cdot (T_H - T_{HW}) \cdot DTM_{HTS\ reactor}}$
DENE	$1 + \dfrac{2 \cdot \Delta H_{evap}}{\Delta H_{r,HTS}}$	$1 + \dfrac{2 \cdot (\Delta H_{NH3} - DTM_{NH3} \cdot (T_{HW} - T_{amb}))}{\Delta H_{r,HTS} + (T_H - T_{abs,HTS}) \cdot DTM_{HTS\ reactor}}$

DRES	$1 + \dfrac{2 \cdot \Delta H_{r,LTS}}{\Delta H_{r,HTS}}$	$1 + \dfrac{2 \cdot \left(\Delta H_{r,LTS} - DTM_{LTS\ reactor} \cdot (T_{HW} - T_{amb}) \right)}{\Delta H_{r,HTS} + \left(T_H - T_{abs,HTS} \right) \cdot DTM_{HTS\ reactor}}$

To use the static models listed in Table 2, the mass and specific heat of various materials are needed. For each unit mass of ammonia absorbed, the mass of salt is determined by the mole ratio of salt and ammonia in the equilibrium reaction formula. The porous matrix material mixed with the sorbent salt does not affect the equilibrium limit of the chemical reaction, but it does add to the DTM of the reactor. In this study expanded graphite (EG) was assumed as the matrix material for all sorbent salts, and the mass ratio of the EG and the salt was set at 35:65 following previous studies (Lépinasse et al. 2001, Bao et al. 2010, Bao et al. 2011a). The specific heat of EG was reported as 0.61 $kJ^1kg^{-1}K^{-1}$ by Bao et al. (2011a). For the mass of reactor metal, Li et al. (2009) estimated the typical mass ratio of the stainless steel reactor to the salt of 5, and in the experimental study of Lepinasse et al. (1994) such mass ratio is 5.6-5.8. Therefore, the mass ratio of 5 was assumed in this study.

Equilibrium properties determine the maximum possible ammonia transferred in each half cycle. The fraction of this actually achieved is dependent on the factors such as reaction rate and cycle time. A realistic reaction completion fraction of 85% was used by Li et al. (2009) in chemisorption refrigeration system models, and this value was assumed in this study. Wang et al. (2009) studied a resorption cycle and pointed out pressure below 0.3 bar during LTS desorption would limit the mass transfer and significantly reduce the cycle capacity. Therefore, a low-pressure limit of 0.5 bar is applied in this study. Additionally, heat production from different vessels is assumed to be at the same temperature. The temperature approach at system boundaries is assumed at 5°C on the refrigerant side and 10°C on the salt reactor side. The cold-climate ambient condition is assumed to be -25°C to 0°C.

In order to compare performance of various systems by using different types of energy resources, primary energy COP is used and defined in equation (7) for the comparison of heating performance of CSHP with other technologies. A conversion ratio of 3.365 is used for electricity to primary energy (Deru and Torcellini 2007). For gas-fired CSHP, the total supplied heat includes the heat from exchangers and the recovered heat in the condensing heat exchanger. Following typical thermal efficiencies of 80% and 95% (higher heating value basis) for non-condensing and condensing furnaces, respectively, in equation (7), the burner efficiency η_{burner} is 0.8, and the condensing heat exchanger efficiency η_{condHX} is 0.15. According to Garrabrant et al. (2016), the ratio of parasitic electricity consumption to gas input is about 4% for condensing furnaces and 6% for GAHP. In this work a ratio of 5% was assumed for CSHP. The operating conditions and assumptions in this study are listed in Table 3.

$$COP_{PE} = \frac{Q_{supply}}{Q_{gas} + 3.15 \cdot P_{electricity}} = \frac{COP_{cycle,ht} \cdot \eta_{burner} + \eta_{condHX}}{1 + 3.15 \cdot P_{electricity}/Q_{gas}} \qquad (7)$$

Table 3: Operating conditions and model assumptions used in this work

T_{HW}, heat supply temperature	50°C
T_{amb}, ambient temperature range	-25°C – 0°C
Temperature approach at refrigerant side (e.g. $T_{amb} - T_{NH3,eq}$)	5°C
Temperature approach at sorbent side (e.g. $T_{amb} - T_{salt,eq}$)	10°C
Cycle pressure limits	>0.5; <50 bar
Matrix material, specific heat, mass ratio matrix:salt	EG, 0.61 $kJ^1kg^{-1}K^{-1}$, 35:65
Exchanger metal, specific heat, mass ratio metal:salt	Stainless steel, 0.46 $kJ^1kg^{-1}K^{-1}$, 5:1
Reaction completion fraction (fraction of maximum ammonia transfer)	0.85
η_{burner}, natural gas burner efficiency (Q_{output}/Q_{gas})	0.80

η_{condHX}, condensing heat exchanger efficiency (Q_{cond}/Q_{gas})	0.15
Primary conversion ratio of electricity	3.15
$P_{electricity}/Q_{gas}$, ratio of CSHP electricity consumption to gas input	0.05

4. ANALYSIS AND DISCUSSION

The first step of chemisorption heat pump design is identifying a cycle configuration and sorbent salts, subject to the constraints of operating conditions. The minimum low-side temperature (T_{Lmin}) is defined as the lowest temperature at which ammonia evaporation or LTS desorption in the CSHP needs to occur to extract heat from low-temperature ambient. Using T_{amb} of -25°C to 0°C and approach temperature of 5°C for ammonia and 10°C for LTS, T_{Lmin} of -35°C to -5°C was investigated. The minimum driving temperatures T_{Hmin} and ideal COP (neglecting DTM) of all available salts using the 4 non-heat-recovery configurations are plotted against the T_{Lmin} in Figure 3. The labeled dots in Figure 3 represent systems with preferable properties such as low required heat source temperature and high ideal COP in their own categories. Since DTM is neglected for ideal COP, the heat recovery cycles have the same ideal COP and constraints as their non-heat recovering counterparts.

For the cycles using ammonia as the low-side material such as SENE and DENE, salts with low operating temperature ranges such as NaBr-5.25NH$_3$ and CaCl$_2$-8NH$_3$ are not able to produce heat at supply temperature under the ammonia evaporation pressure in low-temperature ambient. For those salts with sufficiently high operating temperature ranges, their T_{Lmin} are as low as -30°C. The desorption temperatures of these salts at the higher condensing pressure are used as their T_{Hmin}. For resorption cycles, such as SRES and DRES, however, only three salts with very low operating temperature ranges can be used as LTS under sub-freezing ambient: NH$_4$Cl-3NH$_3$, NaBr-5.25NH$_3$, and PbCl$_2$-8NH$_3$. The lowest temperatures of these LTS are limited by the lower limit of system pressure of 0.5 bar, which is around -23°C for NH$_4$Cl-8NH$_3$, -16°C for PbCl$_2$-8NH$_3$, and -13°C for NaBr-5.25NH$_3$. As a result, the T_{Lmin} of resorption cycles are clustered into these three temperatures corresponding to systems using the three LTS.

Double-effect cycles such as DENE and DRES have three reactant materials, and their operation can be illustrated by Figure 2 (b). The operating pressures are still determined by the low-side material. However, in double-effect cycles, the medium temperature salt (MTS) operates in similar temperature ranges as the single-effect HTS, while the desorption of MTS is driven by the adsorption heat of double-effect HTS. As a result, the operating temperature range of double-effect HTS is even higher than their single-effect counterparts, and in Figure 3 (a) the DENE (red) and DRES (green) tend to require higher source temperatures. Figure 3 (b) illustrates the ideal COP of all available system options. With larger heating output and larger higher reaction heat, the ideal COP of double-effect and resorption cycles tend to be higher than the single-effect cycles with NH$_3$ evaporator. The highest ideal COP for SENE, DENE, SRES, and DRES are 1.51, 1.85, 1.76, and 2.12, respectively. The differences between systems of the same configuration can be attributed to the different reaction enthalpy of various salts.

Once the effects of various dead thermal masses (DTM) are considered, the COP values of all cycle configurations decrease. Figure 4 illustrates the COP of the best-performing working pairs for each configuration considering only inherent thermal mass of the salt and ammonia. Unlike other sorption technologies with continuously variable concentration in their vapor equilibrium, the equilibrium lines of chemisorption are discrete due to the discrete and fixed stoichiometric ratio of salt-ammonia in the chemical reaction formula. Therefore, chemisorption adsorption capacities are agnostic to the temperature lift, and the only factor affected by the varying low-side temperature is the heat loss associated to DTM. As a result, the trends of COP in Figure 4 are all linear with the slope reflecting the effect of DTM. Introducing heat recovery mechanism in single-effect cycles is able to reduce the heat loss of DTM, which leads to raised COP as well as flattened slope indicating less sensitivity to temperature lift. On the other hand, since resorption cycles use twice as much salt compared to cycles with NH$_3$ evaporator, their inherent DTM is higher. This results in more COP reduction from ideal COP as well as a steeper slope indicating more sensitivity to temperature lift.
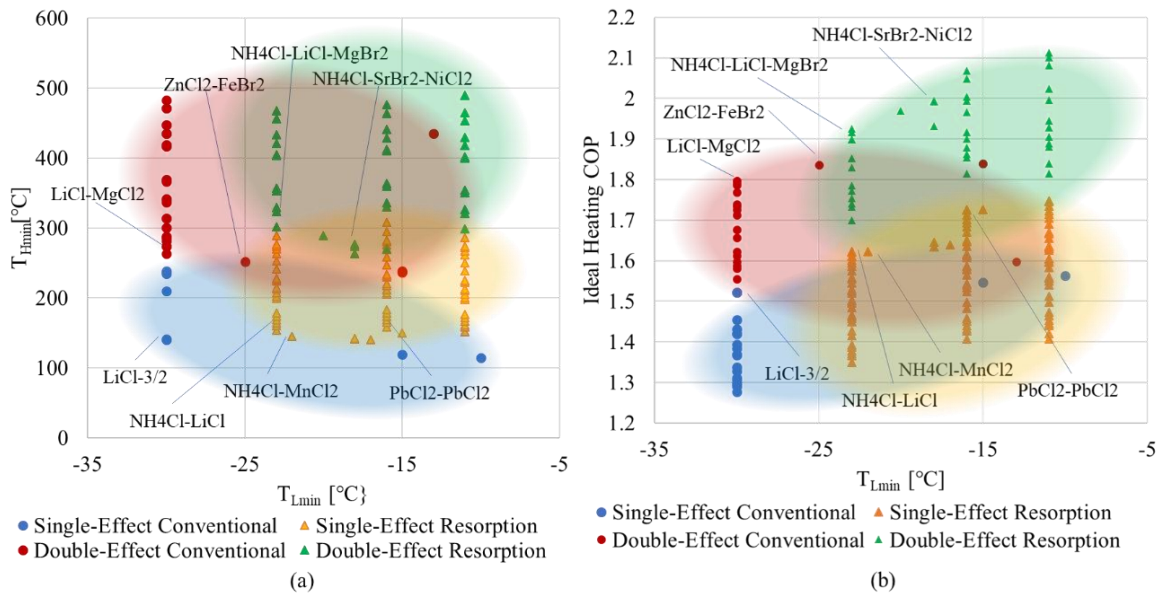
Figure 3: Minimum driving temperature (a) and ideal heating COP (b) of investigated configurations and salts
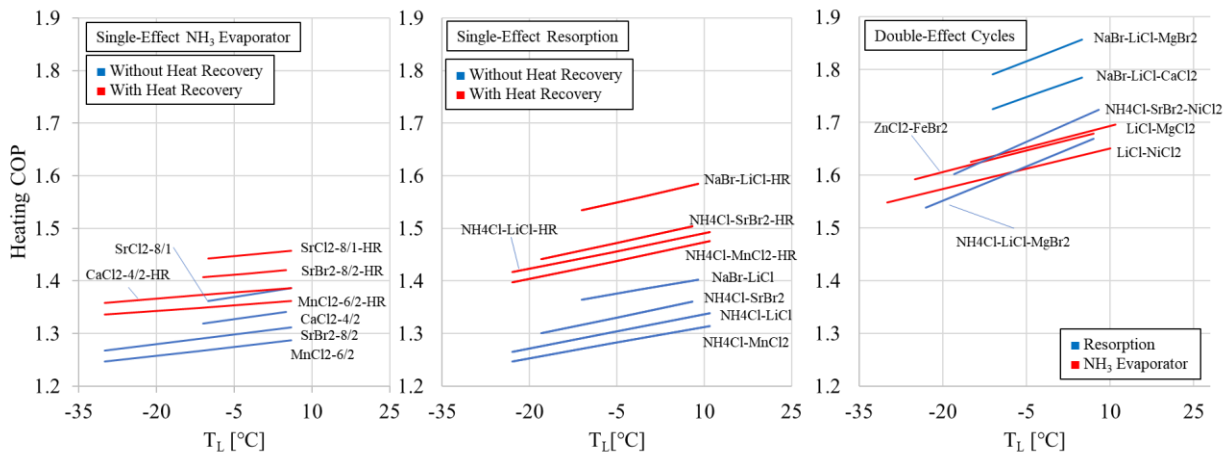

Figure 4: Heating COP of different configurations considering only the inherent thermal mass

The COP of all cycle configurations saw a drop of 0.1-0.4 from the ideal COP depending on the working pair and low-side temperature: single-effect cycles COP lie in the range of 1.25-1.4; for double-effect cycles the range is 1.55-1.85. For the SENE and DENE system, the COP at -15°C are around 1.25 and 1.6, which are slightly higher than the reported value from previous comparison work by Pons et al. (1999). Figure 4 also illustrates the effect of working pair availability based on the $T_{L,min}$: for SENE operating at $T_{L,min}$ below -10°C, $SrBr_2$-8/2NH_3 is the optimal working pair with COP around 1.25-1.31; however, with $T_{L,min}$ above -10°C, $SrCl_2$-8/1NH_3 becomes available and provides higher COP of 1.35-1.4. Similarly for resorption cycles, $NaBr$-5.25NH_3 provides higher COP than NH_4Cl-3NH_3, but is only available when $T_{L,min}$ is above -11°C.

Figure 5 shows the primary energy COP of gas-fired CSHP compared with other heating technologies in the cold-climate temperature range. The COP_{PE} of CSHP in Figure 5 (a) are calculated with DTM assumptions in Table 3, while the COP_{PE} of CSHP in Figure 5 (b) use lower mass ratios for both reactor metal and matrix material, representing possible improved designs. The performance of specially designed cold climate electric heat pumps

(EHP) were from Shen et al. (2016), and single-effect gas-fired absorption heat pump (GAHP) from Garrabrant et al. (2016). The GAHP uses ammonia-water as the working pair and has maintained COP$_{PE}$ around 1.15-1.25 at low ambient. Both the EHP and the GAHP were supplying hot water at 48.8°C. The COP$_{PE}$ of 0.85 for condensing furnace is calculated from gas efficiency of 92% and electricity energy consumption 4% of gas energy consumption. Compared to these technologies, the COP$_{PE}$ of CSHP are less sensitive to the ambient temperature. The best-performing DENE and DRES cycles are able to maintain COP$_{PE}$ of above 1.2 for ambient temperature as low as -20°C. The improvement of design DTM also demonstrated positive influence, especially for DRES cycles.
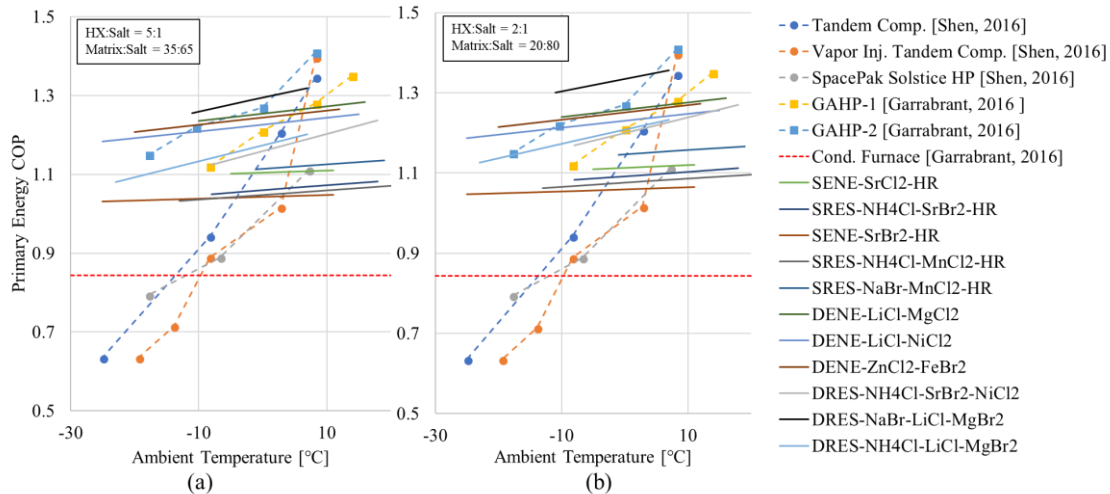

Figure 5: Comparison of single-reaction chemisorption heat pump with other technologies

5. CONCLUSION

In this study, a model-based comparison study involving six cycle configurations and 65 working pairs was carried out on chemisorption systems for cold climate heat pumping applications. Static thermodynamic models were first developed to calculate the heating COP for single- and double-effect resorption/NH$_3$ evaporator cycles. The models account for the effect of thermal mass both intrinsic to the working pair and associated with the system design. The availability and ideal COP under different low temperature constraints were first discussed for combinations of different cycle configuration and working pairs. For the best-performing working pairs in each configuration, the COP considering inherent and design DTM were then calculated using the static model. The DTM had negative impact on the performance of all configurations and especially for resorption cycles, while the single-effect heat recovery cycles were able to alleviate the effect of DTM. Finally, the primary energy COP of the best-performing CSHP systems were calculated. Compared with other cold-climate heat pumping technologies, several CSHP demonstrated sustained COP$_{PE}$ of above 1.2 at ambient temperature below -25°C.

NOMENCLATURE

COP	coefficient of performance	DTM	dead thermal mass [kJ/K]	EG	Expanded graphite
HTS	high temperature salt	HR	heat recovery	LTS	low temperature salt
MTS	medium temperature salt	P	pressure [Pa]	Q	Specific heat flow [kJ/kg NH$_3$]
R	gas constant	T	temperature [K]	ΔH	reaction enthalpy
ΔS	entropy	η	thermal efficiency		
Subscript					
abs	absorption	amb	ambient	cl	cooling
evap	evaporation	eq	equilibrium	H	heat input temperature
ht	heating	HW	heat supply temperature	PE	primary energy
r	reaction	ref	refrigerant	rej	Heat rejection (supply)

ACKNOWLEDGEMENTS

REFERENCES

Bao, H., et al. (2011a). "Working pairs for resorption refrigerator." Applied Thermal Engineering 31(14-15): 3015-3021.

Bao, H. S., et al. (2010). "Choice of Low Temperature Salt for a Resorption Refrigerator." Industrial & engineering chemistry research 49(10): 4897-4903.

Bao, H. S., et al. (2011b). "A resorption refrigerator driven by low grade thermal energy." Energy Conversion and Management 52(6): 2339-2344.

Deru, M., & Torcellini, P. (2007). Source Energy and Emission Factors for Energy Use in Buildings (Revised) (No. NREL/TP-550-38617). National Renewable Energy Laboratory (NREL), Golden, CO..

DOE, U. (2012). Buildings Energy Data Book, 2011. https://openei.org/doe-opendata/dataset/buildings-energy-data-book.

Garrabrant, M., et al. (2016). "Experimental Evaluation of Low-Cost Gas Heat Pump Prototypes for Building Space Heating."

Gluesenkamp, K. (2012). Development and analysis of micro-polygeneration systems and adsorption chillers, University of Maryland, College Park.

Goetz, V., et al. (1993). "The structure and performance of single effect solid-gas chemical heat pumps." Heat Recovery Systems and CHP 13(1): 79-96.

Lepinasse, E., et al. (1994). "Modelling and experimental investigation of a new type of thermochemical transformer based on the coupling of two solid-gas reactions." Chemical Engineering and Processing: Process Intensification 33(3): 125-134.

Lépinasse, E., et al. (2001). "Cooling storage with a resorption process. Application to a box temperature control." Applied Thermal Engineering 21(12): 1251-1263.

Li, T., et al. (2014). "Progress in the development of solid–gas sorption refrigeration thermodynamic cycle driven by low-grade thermal energy." Progress in Energy and Combustion Science 40: 1-58.

Li, T. X., et al. (2009). "A conceptual design and performance analysis of a triple-effect solid–gas thermochemical sorption refrigeration system with internal heat recovery." Chemical Engineering Science 64(14): 3376-3384.

Neveu, P. and J. Castaing (1993). "Solid-gas chemical heat pumps: field of application and performance of the internal heat of reaction recovery process." Heat Recovery Systems and CHP 13(3): 233-251.

Oliveira, R. G., et al. (2008). "Transient analysis of a chemisorption air conditioning system operating under different kinds of cycle." Industrial & engineering chemistry research 47(4): 1102-1110.

Pons, M., et al. (1999). "Thermodynamic based comparison of sorption systems for cooling and heat pumping: Comparaison des performances thermodynamique des systèmes de pompes à chaleur à sorption dans des applications de refroidissement et de chauffage." International Journal of Refrigeration 22(1): 5-17.

Shen, B., et al. (2016). Cold Climate Heat Pumps Using Tandem Compressors, Oak Ridge National Laboratory (ORNL), Oak Ridge, TN (United States). Building Technologies Research and Integration Center (BTRIC).

Wang, L., et al. (2009). "A comparison of the performances of adsorption and resorption refrigeration systems powered by the low grade heat." Renewable Energy 34(11): 2373-2379.

Wang, R., et al. (1998). "Experiments on heat-regenerative adsorption refrigerator and heat pump." International journal of energy research 22(11): 935-941.